ORIGINAL ARTICLE

Ultrasonic micro punching with flexible punch for thin stainless sheet metal

Yan Xiao[1] · Fei Sun[1] · Jia-qi Ran[1] · Bei Wang[1] · Jin-ming Zhong[1] · Jiang Ma[1] · Feng Luo[1]

Abstract

In this paper, an effective ultrasonic-assisted micro-punching method for thin stainless sheet metal with molten plastic as flexible punch is adopted. The minimum micro hole and arrays with diameter of 0.3 mm were punched on rolled state thin stainless sheet metal with a thickness of 10 μm. The deformation mechanism and forming parameter quality were investigated. The experimental results show that cylinder pressure, ultrasonic power, and ultrasonic vibration time were the key parameters which affect each other. The ultrasonic vibration time needed to be properly set up according to the preset cylinder pressure and ultrasonic power to form a complete punching hole and avoid defects or cracks of the parts. For the micro hole with a diameter of 0.6 mm punched on a thin stainless sheet metal with a thickness of 30 μm, there are no significant effects on the qualities of the punching fracture surfaces when changing the punching parameters in the range of the cylinder pressure of 0.3–0.5 MPa and the ultrasonic power of 60–90%. In the case of cylinder pressure 0.5 MPa and ultrasonic power 75%, the width of shearing zone is between 10 and 29%, and the surface roughness Ra of the shearing zone is in the range of 0.10–0.20 μm. Our results could throw light on improving the fracture surface quality of micro-punched part obtained by ultrasonic micro punching with flexible punch.

Keywords Thin stainless sheet metal · Ultrasonic punching · Flexible punch · Micro punching

1 Introduction

Sheet metal micro punching parts have been widely used in precision instruments, electronic equipment, and biomedical and mass consumer goods, and micro-punching technology has received widespread attention. The traditional punching method of rigid punch and die is applied in micro punching and has achieved good research results. J. Xu et al. [1, 2] conducted extensive research on the process parameters, punching quality, size effect, and mold preparation problems of micro punching with mechanical method, and developed a set of micro punching for automatic feeding. The cutting system punched out micro holes and their arrays. G.L. Chern et al. [3] punched out triangular and hexagonal micro holes

with a side length of 0.2 mm on a 100-μm-thick copper sheet, and discussed the method of machining micro punch and micro die with vibration spark technology. B.J. Joo et al. [4] punched out micro holes with a diameter of 25 μm on brass and stainless steel sheets with a thickness of 25 μm, and studied the shear fracture behavior during mechanical punching. Due to the successful application of ultrasound in macro punching, it has also been applied to micro punching by some researchers. T. Takemasu et al. [5] carried out a 40-kHz ultrasonic vibration-assisted mechanical micro punching experiment, and punched out micro holes with a diameter of 0.13 mm on a stainless steel sheet with a thickness of 80–150 μm, and studied the effect of ultrasonic vibration on micro punching. C.J. Wang et al. [6] used 1.0 kHz high-frequency vibration to punch a 0.5-mm square micro hole on a T2 copper sheet with a thickness of 100 μm. Studies have shown that the width of the bright zone increases and the surface roughness decreases after ultrasonic application.

With the decrease of the size of micro-punching parts, the traditional mechanical punching method should solve problems such as micro-punching process, accurate centering of punches and dies, insufficient rigidity of small-sized punches, and easy wear of molds. For micro-hole punching, the flexible

✉ Jiang Ma
majiang@szu.edu.cn

✉ Feng Luo
llf@szu.edu.cn

[1]   Shenzhen Key Laboratory of Advanced Manufacturing Technology for Mold & Die, Shenzhen University, Nanhai Ave. 3688, Shenzhen 518060, Guangdong, People's Republic of China

punch method is a better choice. H. Watari et al. [7] used a polyurethane sheet as a flexible punch to punch a small hole with a diameter of 1.6 mm on a 200-μm-thick aluminum alloy sheet. The punching process of the method was analyzed, and the influence of the thickness and hardness of the polyurethane sheet and the spherical indenter radius of the applied pressure on the punching were studied. J. Sun et al. [8] used polyurethane as a flexible punch and ultrasonically assisted in punching a micro hole with a diameter of 0.8 mm on a 50-μm-thick brass sheet. The depth of the die, the punching force, the punching speed, and the effect of applying ultrasonic on the punching quality were investigated. Y. Kurosaki et al. [9] used a viscoplastic silicon polymer medium as a flexible punch to punch out 3 × 3-Φ50 μm array micro holes on a pure copper sheet with a thickness of 5 μm, and studied the punching parameters on the array micro-hole punching. M. Murata et al. [10] adopting high-pressure gas as a punch to punch pure aluminum and copper sheets with thicknesses of 50 and 100 μm analyzed the punching process under this method, and discussed the effects of gas pressure and die size on the shape accuracy of the hole and the width of the sag zone. The minimum diameter 1 mm hole was obtained. Q.J. Zhao et al. [11] used a single-sided electromagnetic impact forming method to punch out micro holes with a diameter of 0.4 mm on a T2 copper sheet with a thickness of 20 μm, and discussed the effects of thin sheet thickness, impact energy, and discharge time on the quality of micro punching. C. Zheng et al. [12] used a laser shock method to punch micro holes with a diameter of 0.8 mm on a 30-μm-thick brass and pure titanium sheet, and studied the dynamic deformation and fracture behavior of the sheet. H.X. Liu et al. [13] used the laser-flying-driven impact forming method by punching a 0.3-mm square micro hole with a plum-shaped complex contour micro hole with a circumscribed circle diameter of 0.5 mm on an aluminum thin sheet with a thickness of 20 μm, and analyzed the effect of punching parameters on the quality of the punching and the basic characteristics of the method. In addition, the method of combining ultrasonic vibration and flexible punches has also been applied to the micro-forming of thin sheet metal [14].

In this paper, a micro-forming method proposed by our research group, the micro ultrasonic sheet metal forming based on molten plastics as a flexible punch (Micro-USF) is applied to micro-punching. This forming method avoids the difficult problem of punch alignment, so that the punch and die wear are small. Ultrasound can melt the plastic powder to form a fluid flexible punch during the punching process, so that the punching force can be more evenly distributed on the thin sheet, and the fracture surface morphology of the punched parts is similar at different positions on the circumference. There is a big difference of fracture between rigid punching and ultrasonic punching based on molten plastics as a flexible in which the fracture is a kind of fracture under the combined action of pulling and shearing, especially in the last part of the circumference. There is no bright zone on the punched fracture surface, but a shearing zone is formed by material shear slip. There was no significant difference in the quality of the punched fracture surface, when the forming parameters were changed within a certain range.

2 Experimental

2.1 Forming principle

Figure 1 is a schematic diagram of the Micro-USF. The round stock bin is arranged in the middle of the pressure plate, and plastic powder is placed in the stock bin. The thin sheet metal blank and a punching die are placed between the pressure plate and the baseplate, and the pressure plate is fastened to the baseplate by bolts. When punching started, the ultrasonic punch moved down first, and the plastic powder is pressed by the main pressure of the ultrasonic punch, and the ultrasonic vibration is applied after the pressure rises to a preset pressure. The plastic powder repeatedly rubs and collides under the action of ultrasonic vibration, melting into molten plastic which has the properties of viscous fluid medium. As a flexible punch, the molten plastic transmits the pressure and ultrasonic vibration to the thin sheet metal, and forces it to deform and shear, and finally form micro holes. The effect of the ultrasound in the method is that the plastic powder can be melted to form a flexible punch, so that the punching force can be more evenly distributed on the thin sheet. On the other hand, due to the acoustic softening effect of ultrasonic vibration on the blank, the quality of the fracture surface can be improved and the punching force can be reduced [6, 15].
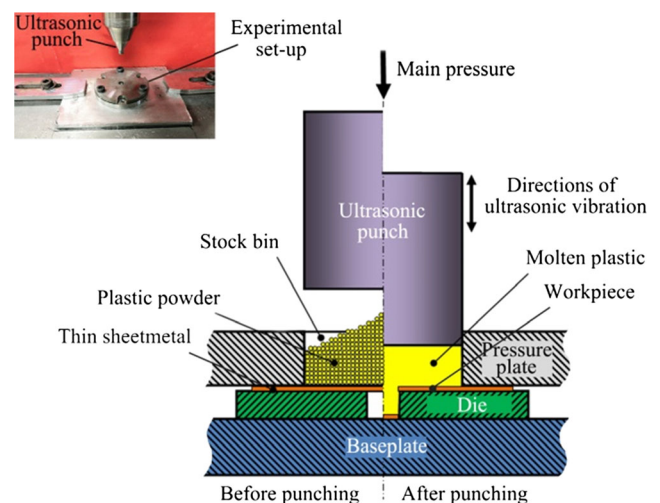

Fig. 1 Schematic diagram of the Micro-USF principle

2.2 Experimental platform

The experimental platform consists of a commercial ultrasonic plastic welder and a set of self-made Micro-USF forming devices. The cylinder pressure built into the ultrasonic welder provides the main pressure of the ultrasonic punch, and the ultrasonic welder is also a device for generating ultrasonic vibration. The experiment adopts 2020 ultrasonic plastic welding machine of Shenzhen Rifa Ultrasonic Equipment Co., Ltd. The main parameters are shown in Table 1. The forming device includes a press plate, a punching die, and a baseplate (see Fig. 1).

In Micro-USF punching, after the ultrasonic vibration is completed, a holding time needs to be set to ensure that the molten plastic solidifies before the ultrasonic head is raised [16]. For Micro-USF, the parameters of the ultrasonic welder can be adjusted, and need to be determined experimentally according to the forming material and forming requirements.

2.3 Punching die

Using the machining method, a circular through hole of $\Phi 0.3$ mm and $\Phi 0.6$ mm and $9 \times \Phi 0.3$ mm array holes are machined on the SKD11 die steel sheet as a punching die with a thickness of 1.2 mm, as shown in Fig. 2.

2.4 Experimental materials

The X10CrNi18-8 cold-rolled stainless steel sheet produced by Pincog, Germany was used as a forming material with thicknesses of 10, 20, and 30 μm, respectively. The chemical comlocation of X10CrNi18-8 stainless steel is shown in Table 2.

Ethylene vinyl acetate copolymer (EVA) plastic powder having an average particle diameter of 350 μm was used as a raw material for the molten plastic flexible punch.

Table 1 Main parameters of Rifa 2020 ultrasonic plastic welding machine

Parameters	Numerical range	Notes
Ultrasonic frequency	20 kHz	Fixed value
Max power	2000 W	Fixed value
Ultrasonic power	50 ~ 100%	Adjustable, interval 1%
Cylinder pressure	0 ~ 0.6 MPa	Continuously adjustable, barometer reading scale 0.02 MPa/grid
Ultrasonic vibration time	0 ~ 9.99 s	Adjustable, interval 0.01 s

3 Results and discussions

3.1 Stainless steel sheet tensile test

The stainless steel sheet is a rolled strip with a width of 50 mm. Using a H-CUT32F medium-wire EDM wire cutter of Shenzhen Liangao Precision Machinery Co., Ltd., the tensile samples are cut along the rolling direction at 0°, 45°, and 90° respectively, as shown in Fig. 3a, where RD: rolling direction, TD: transverse direction. The tensile sample size is shown in Fig. 3b and c is the cut samples.

Tensile test was performed under a Zwick/Roll Z050 stretcher and a Zwick VideoXtens video extensometer at room temperature. Five samples were tested for each direction of the rolled stainless steel sheet with thickness of 30 μm, and the mechanical properties of the obtained stainless steel sheet were shown in Table 3.

The distribution of experimental data of $R_{p0.2}$ and R_m is shown in Fig. 4. Although there are some differences in the data center values in different stretching directions, there are some overlaps in the data distribution intervals of $R_{p0.2}$ and R_m in different stretching directions. Considering the influence of experimental error, it can be considered that the yield strength and tensile strength of rolled stainless steel sheets in different directions are relatively close.

Due to the extremely small thickness of the sample, a small change in the thickness of the sample in the necking stage produces a large stress change, resulting in a rapid increase in stress after R_m. At the same time, the samples in the experiment were not specially treated after cut. The rapidly increasing stress and the small defects of the sample can cause the sample to break quickly after necking, so the measured elongation A_{20mm} is low, the data dispersion is large, and the precision is low.

3.2 The process of micro punching

Micro-USF is a flexible punch micro-punching method. The deformation and fracture process of blank during punching is quite different from the traditional mechanical punching method using a rigid punch. Figure 5 shows the SEM images of a set of samples obtained by terminating the punching process at different times in a micro punching experiment (the SEM photographs of this paper were all taken by an FEI Quanta 450 FEG scanning electron microscope). Figure 5a–d reflect the deformation and fracture of the blank at different times during the micro-punching process. The schematic above the photograph is an analysis of the change in the fracture surface of the blank during the punching process. Figure 5e and f show the occurrence of slippage and micro cracking of the blank relative to the edge location of the punching die before punching. Figure 5g and h are fracture surface topography of micro hole fracture edges prepared by the mosaic method, wherein Fig.

Fig. 2 Punching die. **a** Die mold. **b**–**d** Φ0.6 mm, Φ0.3 mm, and Φ0.3 mm 3 × 3 array local magnification of the micro holes of punching die
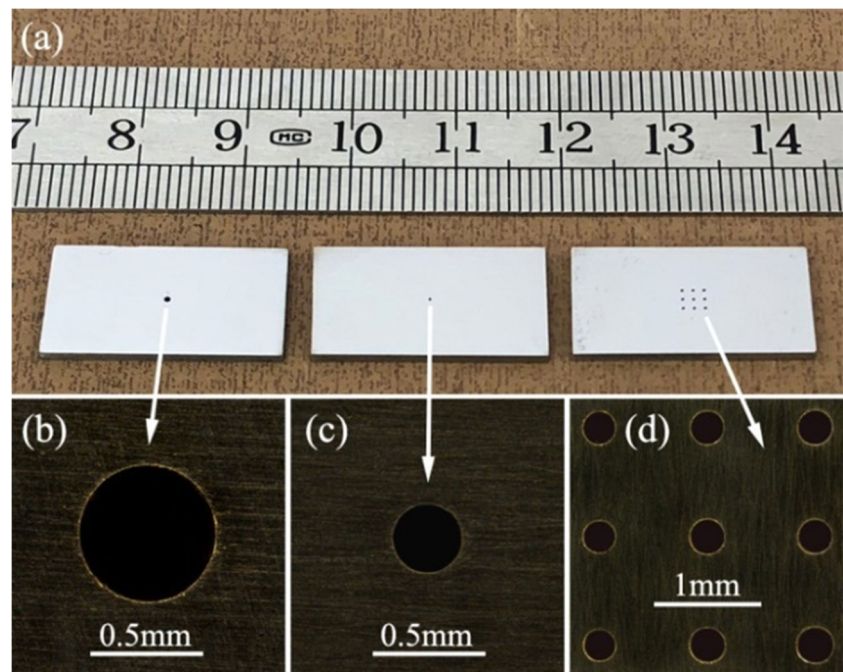
5g and h correspond to fracture surfaces of the earliest and last fracture locations on the edge of a circular hole, respectively.

Figure 5 is a group of typical photographs selected from a large number of experimental samples obtained under different thickness, diameters of punching holes, and experimental parameters, which can best reflect the forming characteristics of the punching process of Micro-USF. As can be seen from Fig. 5, the punch in Micro-USF undergoes these kinds of processes. Firstly, an initial bulging deformation (Fig. 5a) occurred. Then, when the stress of the material reaches the yield strength, the slip line begins to appear, and the lower surface of the blank begins to cut into the hole of the die to produce shear slip (Fig. 5b). Due to the small differences in the force around the circumference of the blank and the local mechanical properties of the material, micro cracks begin to appear on some parts of the circumference of the blank after the stress on the blank reaches the tensile strength (Fig. 5e and f). The micro cracks expand in the direction of the sheet thickness, and the local cracks occur first in the places where the micro cracks are dense (Fig. 5c). The slits extend along the edge of the circular hole and finally merge at some local locations, so that the blanking portion is completely separated from the punching portion to form a complete circular hole (Fig. 5d), and the punching is completed. Therefore, the Micro-USF

process can be divided into four periods, namely, the bulging deformation period (period 1), the micro crack generation period (period 2), the local fracture period (period 3), and the local split which extends circumferentially and completes the punching period (period 4).

Experiments have shown that if ultrasound is not applied, it is difficult to complete all four periods of punching a micro hole having a diameter smaller than 1 mm on a stainless steel sheet with a thickness greater than 10 μm, and it is impossible to punch out the complete micro holes. For thinner sheets and smaller diameter micro holes, the first or second period can only be completed without ultrasound, and on the contrary, it can only be completed to the third period. Applying ultrasonic vibration produces not only an additional ultrasonic force, but also the softening effect of ultrasonic vibration which reduces the yield strength and tensile strength of the material, both of which are beneficial to the completion of punching.

After the local fracture is formed in the third period, the static pressure generated by the cylinder and the ultrasonic additional force are concentrated by the blanking portion to the portion where the hole is not broken. Since the cylinder pressure and the ultrasonic additional force are not reduced, the stress of the unbroken portion increases, which promotes the rapid expansion of the crack along the edge of the circular

Table 2 Chemical composition of X10CrNi18-8 stainless steel (wt%)

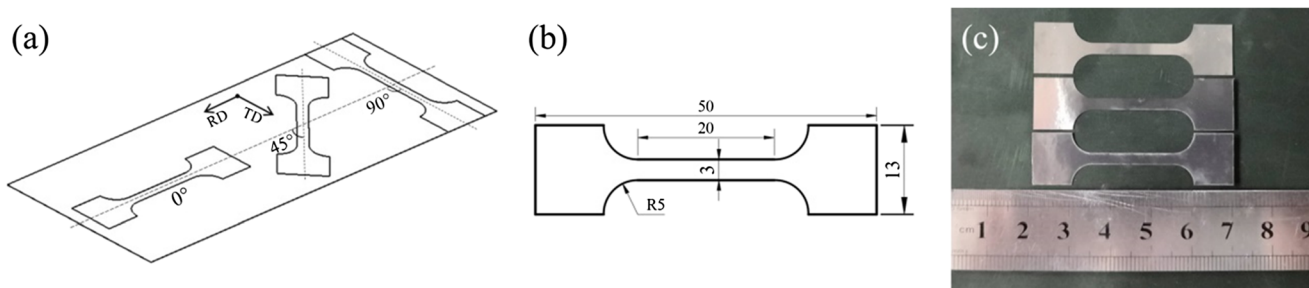|	C	Si	Mn	P	S	N	Cr	Mo	Ni
Chemical composition	0.05 ~ 0.15	≤ 2.00	≤ 2.00	≤ 0.045	≤ 0.015	≤ 0.11	16.00 ~ 19.00	0.80	6.00 ~ 9.50

Fig. 3 Tensile sample. **a** Sample cutting direction. **b** Sample size. **c** Samples

hole. Meanwhile, local cracks may appear at a plurality of locations around the circular hole, as can be seen from Fig. 5c. The initially formed cracks are due to the influence of the tension of the surrounding material, and the burr direction is almost vertically downward along the fracture surface (Fig. 5g), which indicates that these local fractures are in a purely sheared or nearly pure shear fracture mode. At the location of the final fracture, the burr direction is obliquely downward (Fig. 5h), which indicates that at the final junction of the local fracture, the fracture exhibits a kind of compound fracture mode of tensile fracture and shear fracture, due to the lack of tension by the surrounding material.

3.3 Punching parameters

In Micro-USF, cylinder pressure, ultrasonic power, and ultrasonic vibration time are three important punching parameters. Part of the punching force comes from the static pressure generated by the cylinder (the main pressure of the ultrasonic punch), and its magnitude is related to the set cylinder pressure. The other part is derived from the additional force generated by the ultrasound, the magnitude of which is related to the ultrasound power set. The ultrasonic power is expressed as a percentage of the maximum power of 2000 W, for example, 100% means 2000 W and 50% means 1000 W. The setting of ultrasonic vibration time is based on the production of a complete punched hole, which needs to be determined experimentally. In the case that the punched hole has been completed, the excess ultrasonic vibration time is not only

unnecessary, but the ultrasonic vibration causes repeated collision and friction between the formed part and the mold surface, thereby causing damage or even cracking on the surface of the part.

In order to study the reasonable punching parameters, a set of cylinder pressure and ultrasonic power are first set in the experiment, for example, the cylinder pressure is 0.4 MPa, the ultrasonic power is 50%, and then the ultrasonic vibration time is changed at intervals of 0.05 s. Three samples were punched out at each ultrasonic vibration time. When the ultrasonic vibration time is short, the punching cannot be punched through or the blanking and punching cannot be completely separated, that is, the micro punching forming cannot be completed. In the process of increasing the ultrasonic vibration time from small to large, if all of the three samples can be punched out, the time is recorded as the minimum time required to finish the punching. If one of the three samples has surface damage or rupture, the previous time of this time is recorded as the maximum time allowed for the punching. The range between the maximum and minimum time is the available ultrasonic vibration time under this group of cylinder pressure and ultrasonic power.

Table 4 shows the maximum and minimum ultrasonic vibration time of the micro hole with a diameter of 0.6 mm on a stainless steel sheet with a thickness of 30 μm under different cylinder pressures and ultrasonic powers. In the table, "> 9.99" indicates that no damage or cracking occurred even when the ultrasonic vibration time reached the set upper limit. Figure 6 shows the corresponding curve and ultrasonic vibration time interval. When the previous time data of a point is ">

Table 3 Mechanical properties of 30 μm thickness X10CrNi18-8 stainless steel sheet	Direction(°)	Average modulus of elasticity E^a/GPa	Average yield strength $R_{P0.2}$/MPa	Average tensile strength R_m/MPa	Average elongation A_{20mm}/ %
	0	163.02	1362.91	1446.65	0.99
	45	183.22	1299.89	1447.47	0.96
	90	174.92	1351.05	1481.86	1.67

[a] E uses experimentally measured mE values

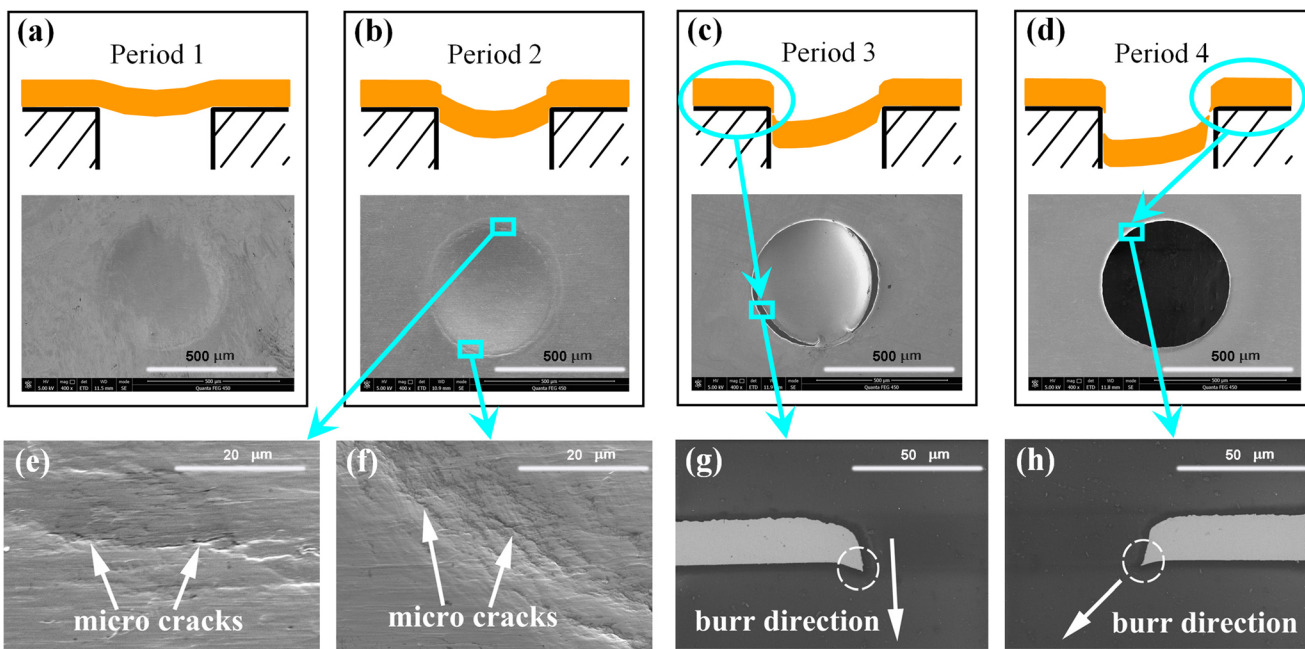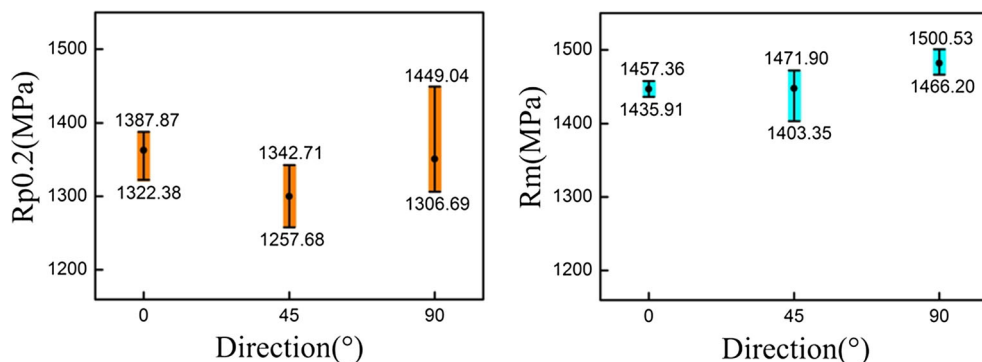**Fig. 4** Data distribution of fracture strength $R_{p0.2}$ and R_m of different samples

Fig. 5 Micro-USF punching process. **a**–**d** Different periods of the punching process. **e** and **f** Local enlargement of the corresponding location of the punching part

9.99," the interval boundary is represented by a vertical virtual image. At the same time, the portion of the ultrasonic vibration time greater than 5 s is cut off in Fig. 6, because the defectless punching hole has been obtained within 5 s.

It can be seen from Table 4 and Fig. 6 that as the cylinder pressure or ultrasonic power increases, both the minimum and maximum times have a trend to decrease. For the minimum time, it is indicated that the ultrasonic

Table 4 Micro-hole punching parameters of thickness 30 μm and diameter 0.6 mm

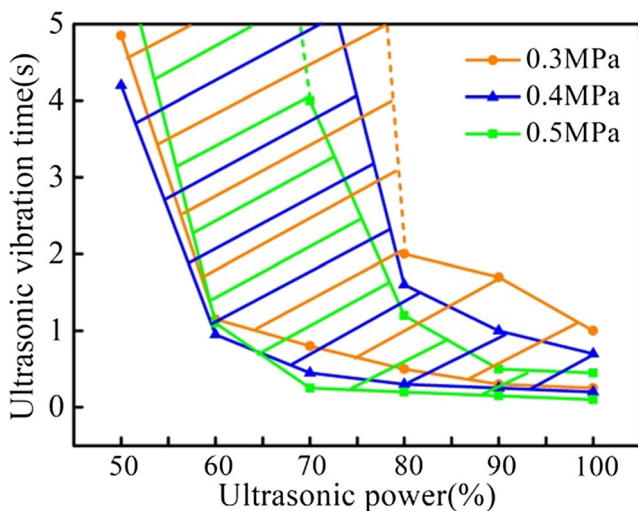| (Unit of ultrasonic vibration time: s)			Ultrasonic power (%)					
			50	60	70	80	90	100
Cylinder pressure (MPa)	0.3	Max time	> 9.99	> 9.99	> 9.99	2.00	1.70	1.00
		Min time	4.85	1.15	0.80	0.50	0.30	0.25
	0.4	Max time	> 9.99	> 9.99	6.50	1.60	1.00	0.70
		Min time	4.20	0.95	0.45	0.30	0.25	0.20
	0.5	Max time	> 9.99	> 9.99	4.00	1.20	0.50	0.45
		Min time	6.00	1.10	0.25	0.20	0.15	0.10

Fig. 6 Ultrasonic vibration time interval of micro-hole punching with thickness 30 μm and diameter 0.6 mm

vibration time for completing the micro-hole punching is shortened as the cylinder pressure or the ultrasonic power is increased. For the maximum time, it indicates that surface damage or cracking is more likely to occur at a larger cylinder pressure or ultrasonic power. Note that in the minimum time, at 0.5 MPa cylinder pressure, there are anomalies in the two data of ultrasonic power 50% and 60%. According to the analysis, this is because under a large pressure, if the ultrasonic power is low and the punching cannot be completed in a short time, the molten plastic as a flexible punch will overflow from the gap between the ultrasonic punch and the pressure plate. As a result, the effective pressure applied to the blank is reduced, so it takes a longer time to complete the punching. When the ultrasonic power is more than 70%, the time required for the punching under a large pressure (0.5 MPa) is extremely short (less than 0.25 s), and the punching has been completed when the molten plastic has not overflowed or only a slight overflow, so the data is restored to normal.

In order to verify this analysis, the minimum ultrasonic vibration time at a cylinder pressure of 0.6 MPa was tested, and the time variation interval used was 0.01 s. At a cylinder pressure of 0.6 MPa, corresponding to ultrasonic power 50%, 60%, 70%, 80%, 90%, and 100%, the minimum ultrasonic vibration time was > 9.99 s, 1.15 s, 0.28 s, 0.22 s, 0.15 s, and 0.10 s, respectively. Compared with the experimental data of cylinder pressure of 0.5 MPa, in the interval of ultrasonic power 50 ~ 80%, the minimum ultrasonic vibration time of 0.6 MPa at the same ultrasonic power increases, that is, the minimum required ultrasonic vibration time is longer and abnormal when the cylinder pressure is increased. When the ultrasonic power is 50%, the punching cannot be completed even at the upper limit of the settable ultrasonic vibration time. At the same time, the ultrasonic power interval where the ultrasonic vibration time is abnormal at 0.6 MPa is also expanded, from 50 ~ 60% at 0.5 MPa to 50 ~ 80%. Thus, experiments showed that the larger the cylinder pressure, the more severe the molten plastic overflow phenomenon, and the faster the effective pressure applied to the blank decreases, so the longer ultrasonic vibration time was needed. It was also observed in the experiment that the larger the cylinder pressure, the more the molten plastic overflows and the faster the overflow rate.

Figure 7 is micro-hole samples punched out by the Micro-USF method, of which: *t*-thickness of sheet metal, *d*-diameter of hole, *CP*-cylinder pressure, *UP*-ultrasonic power, *UT*-ultrasonic vibration time.

3.4 Punching fracture surface

Figure 8 is a 1/4 circumferential fracture surface view of a Micro-USF punched micro hole from a parallel (0°) to a perpendicular (90°) on the rolling direction. In the figure, RD is the rolling direction, TD is the transverse direction, and the angle value is the angle formed by the fracture surface and the rolling direction.

The fracture surface section is made up of a rollover zone, a shearing zone, a fracture zone, and a burr, as shown in Fig. 9. Since the Micro-USF uses a flexible punch, there is no rigid punched burnish zone. Although the stainless steel sheet used in the experiment is in a rolled state, it is anisotropic. However, experimental

Fig. 7 Stainless steel sheet Micro-USF punching samples. **a** *t* = 30 μm, *d* = 0.6 mm, *CP* = 0.4 MPa, *UP* = 75%, *UT* = 0.45 s. **b** *t* = 10 μm, *d* = 0.3 mm, *CP* = 0.4 MPa, *UP* = 70%, *UT* = 0.20 s. **c** *t* = 10 μm, *d* = 0.3 mm, 3 × 3 array holes, distance of hole center = 1 mm, *CP* = 0.4 MPa, *UP* = 70%, *UT* = 0.30 s
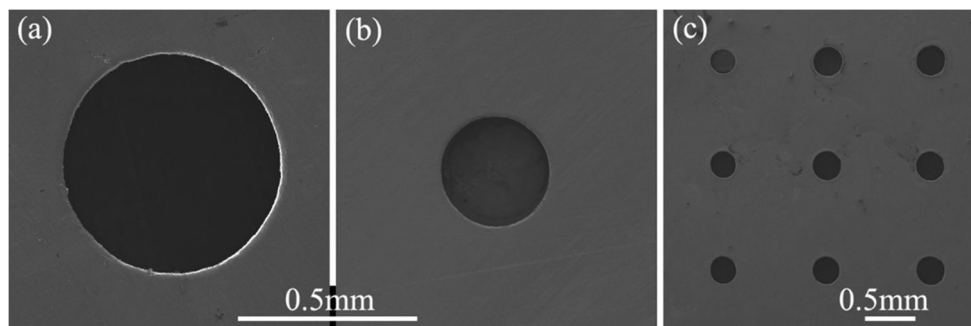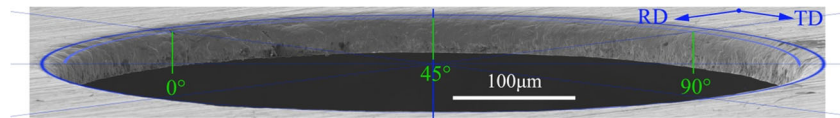
Fig. 8 Punching fracture surface: $t = 30$ μm, $d = 0.6$ mm

observations show that a large number of fractured dimples appear in the parallel and perpendicular to the rolling direction, and in the other directions between the parallel and vertical directions, and the dimples are elongated along the downward direction of the fracture surface. It is shown that the fractures around the circumference are all a ductile shear fracture. The fracture surfaces at different positions on the circumference have similar characteristics, which is the result of the close mechanical properties in all directions of the thin sheets.

Table 5 compares the fracture surface of three typical locations, such as 0°, 45°, and 90°, with a diameter of 0.6 mm micro hole on a 30-μm stainless steel sheet with different punching parameters. In the table, RZ-rollover zone, SZ-shearing zone, FZ-fracture zone, Bu.-burr, the corresponding values are the percentages of the zones measured on the symmetry center line of the photograph. The ultrasonic vibration time used for forming each sample in the table is slightly larger than the minimum ultrasonic vibration time determined in Table 4 or Fig. 6, in order to obtain a good punching sample.

It can be seen from Fig. 9 that at different locations on the fracture surface, even in the very close location, the width of each zone shows a large difference. At the same time, the demarcation points of each zone are also difficult to define accurately. Therefore, the width of each zone in Table 5 is only a rough value.

The widths of the zones on the fracture surface at different locations of the circumference show a large difference. According to the analysis, the force around the round hole is not exactly the same as that in the punching process, so the shear slip speed and the pressure perpendicular to the cut surface are different, and the order of the breaks is different. Therefore, the morphology of the fracture surface at different
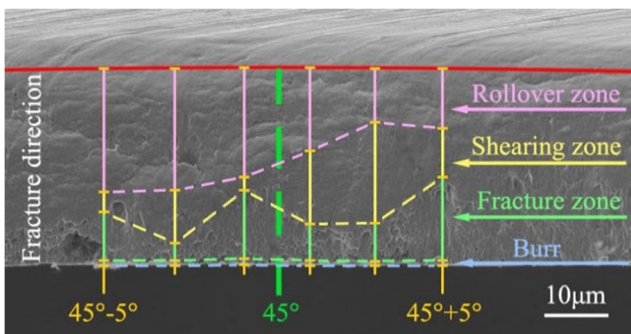
locations has a large randomness. Even samples formed under the same parameters showed significant differences at their corresponding locations, as shown in Table 5 for group A comparison. Considering the randomness factor of such fracture surface formation, the fracture surface morphology did not change significantly when the punching parameters were changed, as shown in Table 5 for comparison of group B and group C samples.

Comparing the 0° and 90° fracture surface of each sample, it can be seen that, in general, the 0° location fracture surface exhibits large irregularities, and the slip marks forming the rollover zones are relatively disordered, and the rollover zones are large. The 90° location fracture surface is more regular, which is mainly affected by the rolling direction.

The roughness Ra of each zone of the sample's fracture surface was measured using a Keyence VK-X250K laser scanning confocal microscope, as shown in Table 6. Sample 7 measures the roughness at each of the 1/4 circumferences at 15° intervals, and each measurement location is measured at three nearby locations. Figure 10 shows the corresponding curve of sample 7. For comparison, the roughness of the 45° location in sample 8 of different parameters was measured.

4 Conclusion

Micro holes were carried out on rolled stainless steel sheets using the Micro-USF method. The main conclusions are as follows:

1. Micro-USF is another method which can make micro holes on thin sheet metal besides of the other existing punching methods.
2. There is a big difference between this punching forming process and the rigid punching. The fracture is a kind of fracture under the combined action of pulling and shearing, especially in the last part of the circumference, and the combined action of pulling and shearing is more significant.
3. The mechanical properties of the rolled stainless steel sheets are close to each other in all directions. Therefore, the fracture surface morphology of the punched holes at different angles from the rolling direction is similar, and both exhibit ductile fracture characteristics. However, the distribution of each zone on the

Fig. 9 Each zone of the punching fracture surface

Table 5 The fracture surface comparison of punched micro hole with thin stainless sheet metal thickness 30 μm and diameter 0.6 mm

Comparative group	Sample No.	Punching parameters		Locations											
		CP (MPa)	UP (%)	0 °				45 °				90 °			
				RZ (%)	SZ (%)	FZ (%)	Bu. (%)	RZ (%)	SZ (%)	FZ (%)	Bu. (%)	RZ (%)	SZ (%)	FZ (%)	Bu. (%)
Group A: same CP and UT	1	0.3	60												
				37	31	32	10	33	29	38	9	32	23	45	9
	2														
				31	19	50	8	31	30	39	10	28	24	48	11
Group B: different CP with same UT	3	0.3	75												
				34	24	42	10	30	33	37	7	36	15	49	10
	4	0.4													
				37	17	46	9	51	13	36	7	41	10	49	8
	5	0.5													
				40	10	50	10	38	29	33	8	29	25	46	9

Table 5 (continued)

Group C: same CP with different UT	1	0.3	60			
				37	31	32	10	33	29	38	9	32	23	45	9
	3		75			
				34	24	42	10	30	33	37	7	36	15	49	10
	6		90			
				33	11	56	13	29	39	32	11	29	34	37	9

circumference is affected by the local force difference and the order of fracture, etc., showing a large unevenness and randomness.

4. When the diameter of 0.6 mm micro hole was punched out on the rolled stainless steel sheet with a thickness of 30 μm, the punching fracture surface was not significantly different in the range of the punching forming parameters of cylinder pressure 0.3–0.5 MPa and ultrasonic power 60–90%.

5. Different from rigid punching, there is no bright zone on the punched fracture surface, but a shearing zone is formed by material shear slip. In the case of a cylinder pressure of 0.5 MPa and an ultrasonic power of 75%, the shearing zone width is between 10 and 29%, and the surface roughness Ra is in the range of 0.10–0.20 μm.

6. The ultrasonic vibration time as an important punching parameter, it is unnecessary to continue applying the ultrasound after a hole has been punched up. Excessive

Table 6 Roughness Ra of each fracture surface of the sample, unit: μm

| Sample no.	CP (MPa)	UP (%)	Location (°)	RZ (μm)	SZ (μm)	FZ (μm)
7	0.5	75	0	0.69 (+ 0.08, − 0.10)	0.14 (+ 0.10, − 0.06)	0.25 (+ 0.07, − 0.05)
			15	0.63 (+ 0.15, − 0.18)	0.16 (+ 0.08, − 0.06)	0.34 (+ 0.15, − 0.11)
			30	0.56 (+ 0.12, − 0.10)	0.15 (+ 0.15, − 0.08)	0.27 (+ 0.04, − 0.04)
			45	0.39 (+ 0.12, − 0.18)	0.12 (+ 0.11, − 0.06)	0.33 (+ 0.05, − 0.04)
			60	0.69 (+ 0.20, − 0.12)	0.13 (+ 0.07, − 0.08)	0.31 (+ 0.13, − 0.08)
			75	0.56 (+ 0.17, − 0.10)	0.20 (+ 0.10, − 0.09)	0.31 (+ 0.07, − 0.09)
			90	0.56 (+ 0.15, − 0.08)	0.14 (+ 0.04, − 0.05)	0.28 (+ 0.09, − 0.06)
			Average	0.58 (+ 0.11, − 0.20)	0.15 (+ 0.05, 0.03)	0.30 (+ 0.04, − 0.05)
8	0.3	75	45	0.48 (+ 0.09, − 0.11)	0.10 (+ 0.04, − 0.05)	0.31 (+ 0.02, − 0.04)
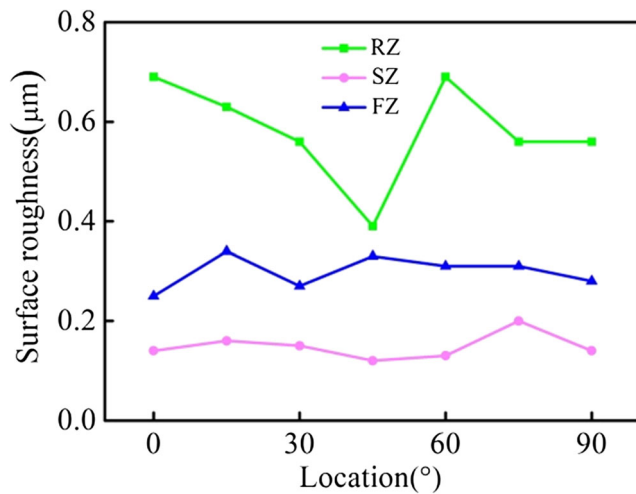
Fig. 10 Roughness of each zone of the punching fracture surface (sample 7)

elongating ultrasonic vibration time may cause surface defects or even cracks of the part. Therefore, the ultrasonic vibration time is preferably slightly higher than the lower limit of the forming time interval.

References

1. Xu J, Guo B, Shan DB, Wang CJ, Li J, Liu YW, Qu DS (2012) Development of a micro-forming system for micro-punching process of micro-hole arrays in brass foil. J Mater Process Technol 212(11):2238–2246

2. Xu J, Guo B, Shan DB, Wang ZL, Li MX, Fei X (2014) Micro-punching process of stainless steel foil with micro-die fabricated by micro-EDM. Microsyst Technol 20(1):83–89

3. Chern GL, Wang SD (2007) Punching of noncircular micro-holes and development of micro-forming. Precis Eng 31(3):210–217

4. Joo BY, Rhim SH, Oh SI (2005) Micro-hole fabrication by mechanical punching process. J Mater Process Technol 170(3):593–601

5. Takemasu T, Yamasaki S, Miura H, Mizue R, Hoshiyama T, Ozaki T (2006) Piercing process by punch striking using ultrasonic vibration trial construction of experimental apparatus and forming property of microholes. J JSTP 47(548):81–85

6. Wang CJ, Guo B, Shan DB, Qin Y (2015) Investigation into high-frequency-vibration assisted micro-blanking of pure copper foils. MATEC Web Conf 21:09004-1-09004-7

7. Watari H, Ona H, Yoshida Y (2003) Flexible punching method using an elastic tool instead of a metal punch. J Mater Process Technol 137(1-3):151–155

8. Sun J, Zhou SN, Yang XL, Xing YJ, Liu X (2016) Polyurethane-rubber punching process for micro-hole arrays. Microsyst Technol 23(7):2943–2950

9. Kurosaki Y, Furukawa Y (1989) Studies on microplastic working (one-shot piercing of many fine holes by VM process). Trans Jpn Soc Mech Eng Ser C 55(516):2206–2212

10. Murata M, Uede Y, Suzuki H (1995) Punchless punching of thin sheet metal by ultrahigh pressure gas for circular hole. J Mater Process Technol 48(1):59–68

11. Zhao QJ, Xu J, Wang CJ, Shan DB, Guo B (2015) Electromagnetic micro-punching process of T2 copper foil. Adv Mater Res 1120-1121:1220–1225

12. Zheng C, Ji Z, Song LB, Fu J, Zhu YH, Zhang JH (2015) Variation of fracture mode in micro-scale laser shock punching. Opt Laser Technol 72:25–32

13. Liu HX, Lu MM, Wang X, Shen ZB, Gu CX, Gu YX (2015) Micro-punching of aluminum foil by laser dynamic flexible punching process. Int J Mater Form 8(2):183–196

14. Zhong JM, Luo F, Wu XY, Hu YF, Xu B, Ling SQ, Li JB (2015) Ultrasonically driven molten resin bulge for the formation of metal micro-structures in laminated die cavity. Int J Adv Manuf Technol 76:1845–1853

15. Witthauer AT, Kim GY, Faidley LE, Zou QZ, Wang Z (2014) Effects of acoustic softening and hardening in high-frequency vibration-assisted punching of aluminum. Mater Manuf Process 29(10):1184–1189

16. Luo F, Wang B, Li ZW, Wu XY, Gong F, Peng TJ, Li KH (2017) Time factors and optimal process parameters for ultrasonic microchannel formation in thin sheet metals. Int J Adv Manuf Technol 89:255–263